

RESEARCH

Open Access



# Orai1 and Orai3 act through distinct signalling axes to promote stemness and tumorigenicity of breast cancer stem cells

Duan Zhuo<sup>1,2†</sup>, Zhenchuan Lei<sup>1,2†</sup>, Lin Dong<sup>3</sup>, Andrew Man Lok Chan<sup>1</sup>, Jiacheng Lin<sup>1</sup>, Liwen Jiang<sup>4</sup>, Beibei Qiu<sup>5</sup>, Xiaohua Jiang<sup>1</sup>, Youhua Tan<sup>6</sup> and Xiaoqiang Yao<sup>1,2,4\*</sup> 

## Abstract

**Background** One of major challenges in breast tumor therapy is the existence of breast cancer stem cells (BCSCs). BCSCs are a small subpopulation of tumor cells that exhibit characteristics of stem cells. BCSCs are responsible for progression, recurrence, chemoresistance and metastasis of breast cancer. Ca<sup>2+</sup> signalling plays an important role in diverse processes in cancer development. However, the role of Ca<sup>2+</sup> signalling in BCSCs is still poorly understood.

**Methods** A highly effective 3D soft fibrin gel system was used to enrich BCSC-like cells from ER+ breast cancer lines MCF7 and MDA-MB-415. We then investigated the role of two Ca<sup>2+</sup>-permeable ion channels Orai1 and Orai3 in the growth and stemness of BCSC-like cells in vitro, and tumorigenicity in female NOD/SCID mice in vivo.

**Results** Orai1 RNA silencing and pharmacological inhibition reduced the growth of BCSC-like cells in tumor spheroids, decreased the expression levels of BCSC markers, and reduced the growth of tumor xenografts in NOD/SCID mice. Orai3 RNA silencing also had similar inhibitory effect on the growth and stemness of BCSC-like cells in vitro, and tumor xenograft growth in vivo. Mechanistically, Orai1 and SPCA2 mediate store-operated Ca<sup>2+</sup> entry. Knockdown of Orai1 or SPCA2 inhibited glycolysis pathway, whereas knockdown of Orai3 or STIM1 had no effect on glycolysis.

**Conclusion** We found that Orai1 interacts with SPCA2 to mediate store-independent Ca<sup>2+</sup> entry, subsequently promoting the growth and tumorigenicity of BCSC-like cells via glycolysis pathway. In contrast, Orai3 and STIM1 mediate store-operated Ca<sup>2+</sup> entry, promoting the growth and tumorigenicity of BCSC-like cells via a glycolysis-independent pathway. Together, our study uncovered a well-orchestrated mechanism through which two Ca<sup>2+</sup> entry pathways act through distinct signalling axes to finely control the growth and tumorigenicity of BCSCs.

**Keywords** Breast cancer stem cells, Orai1, Orai3, Glycolysis

<sup>†</sup>Duan Zhuo and Zhenchuan Lei contributed equally as co-authors of this article.

\*Correspondence:

Xiaoqiang Yao  
yao2068@cuhk.edu.hk

Full list of author information is available at the end of the article



## Introduction

Breast cancer is the most frequently happened malignancy in women [1]. Although there has been great improvement in breast cancer treatment, breast cancer mortality is still high partly due to the existence of breast cancer stem cells (BCSCs) that are resistant to current therapies. BCSCs are the highly tumorigenic cancer cells, and they also possess self-renewal, metastatic and drug-resistant properties [2]. Therefore, advancing our understanding on BCSCs is crucial for developing new breast cancer therapies.

Orai proteins, including Orai1 to Orai3, are  $\text{Ca}^{2+}$ -selective ion channels mediating  $\text{Ca}^{2+}$  entry [3]. Orai1 proteins contain functional domains in N- and C-termini that can interact with other proteins such as stromal interaction molecule 1 (STIM1) and the secretory pathway  $\text{Ca}^{2+}$ -ATPase 2 (SPCA2) [4]. In most cell types, Orai1 mediates store-operated  $\text{Ca}^{2+}$  entry (SOCE), in which depletion of intracellular stores is sensed by  $\text{Ca}^{2+}$  sensor STIM1 located in the endoplasmic reticulum to activate Orai1 in the plasma membrane [5]. However, in estrogen receptor-positive (ER+) breast cancer cells, SOCE is mediated by Orai3-STIM1 [6], whereas Orai1 interacts with SPCA2 to form a signaling complex mediating store-independent  $\text{Ca}^{2+}$  influx (SICE) [7]. Intriguingly, Orai1-SPCA2-mediated SICE in mammary acinar cells is important for high-throughput  $\text{Ca}^{2+}$  transport from maternal blood to milk during lactation [4, 7].

Orai1 and Orai3 also play important functional roles in breast cancer [3, 8]. The expression levels of Orai1 and/or Orai3 are often upregulated in human breast cancer [3, 9]. Mechanistically, Orai1 and Orai3 promote breast cancer cell proliferation [7, 10], migration and invasion *in vitro* [6, 11], and tumor growth and metastasis *in vivo* [3, 7–11]. However, none of these previous studies have investigated Orai1 and Orai3 in the context of BCSCs. The role of Orai1 and Orai3 in BCSCs is poorly understood.

Metabolic phenotype is a crucial determinant of BCSC properties, influencing tumorigenesis, metastasis, drug resistance and tumor relapse [12]. Therefore, targeting BCSC metabolism has been a recent hot strategy for breast cancer therapy [12, 13]. One unique characteristic of BCSCs is their metabolic flexibility. BCSCs can switch between oxidative phosphorylation and glycolysis dependent on cancer microenvironment [12]. However, in general, BCSCs strongly favor the glycolysis pathway [12, 14].  $\text{Ca}^{2+}$  signaling is a well-known regulator of cancer cell metabolism [15]. However, up to the present there is still lack of information about the role of  $\text{Ca}^{2+}$  signaling in the regulation of glycolysis in cancer stem cells (CSCs).

In the present study, we employed a highly effective 3D soft fibrin gel method [16, 17] to enrich BCSC-like cells from ER+MCF7 cell line and MDA-MB-415 cell line. When cultured within these gels, single cancer cells from human cancer cell lines can grow within a few days into individual tumor spheroids that resembled stem cell embryonic bodies [16, 17]. This method offers great advantage over conventional stem cell marker-based CSC enrichment methods, because CSC markers are often unreliable [16, 17]. Indeed, the CSCs enriched by 3D soft fibrin gel demonstrate remarkable tumorigenicity [16, 17]. As few as 10 such selected murine B16-F1 melanoma cells are already capable of forming a tumor and metastasizing to lung [16, 17]. Herein, we utilized the BCSC-like cells enriched by this method to investigate the role of Orai1 and Orai3 in BCSCs. We hypothesized that Orai1-SPCA2 mediates SICE to promote the growth and tumorigenicity of BCSC-like cells via glycolysis pathway, whereas Orai3-STIM1 mediates SOCE to promote the growth and tumorigenicity of BCSC-like cells via a glycolysis-independent pathway. A variety of methodologies, including tumor spheroid growth in 3D soft fibrin gel, cytosolic  $\text{Ca}^{2+}$  measurement, tumor xenograft growth in NOD/SCID mice, RT-qPCR and immunoblots, were used to test these hypotheses.

## Materials and methods

### Reagents

Paclitaxel, fluorouracil (5-fu), collagenase, dispase II,  $\beta$ -Estradiol and cyclopiazonic acid (CPA) were from Sigma-Aldrich. 2-deoxy-D-glucose (2-DG) was from Alfa Aesar. Puromycin and blasticidin were from InvivoGen. Polybrene was from Santa Cruz. Fluo-4/AM were from Invitrogen. AnCoA4 was from Merck Millipore. RO 2959 were from AOBIOUS. Salmon fibrinogen and thrombin were from Searun Holdings.

### Animals and cell lines

The work has been reported in line with the ARRIVE guidelines 2.0. All experimental mice were kept in SPF-grade animal facilities in the Laboratory Animal Service Center of The Chinese University of Hong Kong. Female NOD/SCID mice were housed in SPF-level mouse facilities and raised until 4–5 weeks of age for experimental use. The experiment on mice was approved by the Animal Experimental Ethics Committee of The Chinese University of Hong Kong.

Human breast cancer cell lines MCF7, MDA-MB-415 and human embryonic kidney (HEK) 293 FT cells were purchased from ATCC and were cultured in DMEM (Gibco) supplemented with 10% fetal bovine serum (FBS; Gibco) and 1% penicillin–streptomycin (PS; Gibco).

### Cell culture in 3D soft fibrin gel

3D soft fibrin gels were prepared as described previously [16]. Briefly, salmon fibrinogen (Searun Holdings) was diluted to 2 mg/ml using T7 buffer (50 mM Tris, 150 mM NaCl, pH7.4). Then, fibrinogen was mixed with the cell suspension at a ratio of 1:1, resulting in 1 mg/ml (90 Pa) fibrinogen. Next, 50  $\mu$ l fibrinogen/cell mixture was seeded in one well of 96-well plate and mixed with pre-added 1  $\mu$ l thrombin (100 U/ml, Searun Holdings). The plate was incubated in a humidified incubator (37 °C, 95% O<sub>2</sub> and 5% CO<sub>2</sub>) for at least 15 min to solidify before adding 150  $\mu$ l DMEM (with FBS and PS). Culture medium was changed every two days. Starting from day2, at least 30 colonies and two wells were recorded per condition every two days by Olympus IX83 Inverted Microscope.

### siRNA transfection, RNA isolation and RT-qPCR

siRNA transfection was performed using lipofectamine RNAiMAX transfection reagent (ThermoFisher) following the manufacturer's protocol. To improve the transfection efficacy, we performed transfection when cell confluency reached to 60%-80%. Meanwhile, PS was removed from the culture medium during transfection and re-introduced 72 h post-transfection.

Total RNA was isolated using RNeasy Micro Kit (Qiagen) following the manufacturer's protocol. The RNA concentration was measured using a NanoDrop 2000 Spectrophotometer. 1  $\mu$ g RNA was used for cDNA synthesis using High Capacity cDNA Reverse Transcription Kit (Applied Biosystems) at the condition of 25 °C for 10 min, 37 °C for 120 min and 85 °C for 5 min in a PCR machine.

Reverse transcription-quantitative polymerase chain reaction (RT-qPCR) was conducted using a quantitative SYBR Green Select Master Mix (Applied Biosystems) in 7900HT Fast Real-Time PCR System (Applied Biosystems). The RT-qPCR reactions were run under the following conditions: initial denaturation at 95 °C for 10 min, followed by 40 cycles of denaturation at 95 °C for 15 s, annealing and extension at 60 °C for 1 min. A melting curve analysis was subsequently performed, consisting of 95 °C for 15 s, 60 °C for 15 s and 95 °C for 15 s. Triple wells were included for each sample. The mRNA levels of the targeted genes were normalized to  $\beta$ -actin and expressed with the  $2^{-\Delta\Delta CT}$  method [18, 19]. All primer sequences are listed in Table S1.

### Plasmids transfection, shRNA lenti-viral vector packaging and infection

Plasmid transfection was performed using lipofectamine 2000 (Invitrogen) according to the manufacturer's protocol. shRNA constructs were co-transfected with psPAX2

and pMD2.G at a ratio of 4:3:1 to HEK293 FT cells to generate lentivirus. After 48 h and 72 h, the culture medium was harvested, centrifuged and added to MCF7 cells in the presence of 10  $\mu$ g/ml polybrene (Santa Cruz). 2  $\mu$ g/ml puromycin (Orai1 and STIM1) or 16  $\mu$ g/ml blasticidin (Orai3) were used to select stably knockdown cell lines [20]. Targeted sequences are listed in Table S2.

### Glucose uptake assay, pyruvate and lactate level measurement

Cells were starved for 1 h in glucose-free medium, followed by incubating with 300  $\mu$ M 2-(*N*-nitrobenz-2-oxa-1,3-diazol-4-yl)amino (2-NBDG; ThermoFisher) for 30 min. Then, fibrin gel was dissolved by collagenase (Sigma) and dispase II (Sigma) [21]. Colonies were collected and pipetted into single cells. Finally, 2-NBDG uptake level was measured by flow cytometry.

Cell culture medium was collected. Pyruvate production and lactic acid level were measured using pyruvate assay kit (Nanjing Jiancheng Bioengineering Institute) and lactic assay kit (Nanjing Jiancheng Bioengineering Institute) following the manufacturer's protocol. All values were normalized to protein concentration.

### Western blotting

Detailed methods were described elsewhere [22, 23]. Briefly, cells were lysed by RIPA lysis buffer (Beyotime) containing 1 mM PMSF (Beyotime) on ice for 30 min. The protein concentration was measured using an Enhanced BCA Protein Assay Kit (Beyotime). The protein supernatant was directly boiled in SDS loading buffer for 5 min at 95 °C.

Equal amounts (25–50  $\mu$ g/lane) of protein were separated by 10% SDS-PAGE gel (Bio-Rad) at 80 V for 30 min and then at 120 V for 90–120 min. The protein on the gel was transferred to polyvinylidene fluoride membranes (PVDF; Bio-Rad) at 300 mA for 90 min. The membranes were then blocked with 4% BSA, incubated with diluted primary antibodies to Orai1 (1:1000, Proteintech), GAPDH (1:5000, Proteintech),  $\beta$ -actin (1:5000, Proteintech), STIM1 (1:1000, Alomone Labs) and SPCA2 (1:200, Santa Cruz) overnight at 4 °C. Proteins were visualized using an HRP-conjugated secondary antibody (GE Healthcare) and imaged using ECL Western Blotting Detection Reagents (Amersham). Quantification was performed using ImageJ.

### Cytosolic Ca<sup>2+</sup> measurement

Cytosolic Ca<sup>2+</sup> measurement was performed as described previously [24]. Briefly, cells were loaded with fluo-4/AM and incubated for 30 min. For SICE (or basal Ca<sup>2+</sup> influx) measurement, the cells loaded with Fluo-4/AM

were buffered in a calcium-free physiological saline solution (calcium-free PSS), which contained 140 mM NaCl, 5 mM KCl, 2 mM MgCl<sub>2</sub>, 5 mM HEPES, 10 mM glucose, PH 7.4, followed by adding 2 mM Ca<sup>2+</sup> to induced Ca<sup>2+</sup> entry. For SOCE measurement, cells loaded with Fluo-4/AM were buffered in calcium-free PSS. Then, 10 μM CPA was added to deplete Ca<sup>2+</sup> stores, followed by adding back of 2 mM Ca<sup>2+</sup> to trigger SOCE. The fluo-4 fluorescence signals were recorded using FV1000 laser scanning confocal imaging system at excitation/emission of 488/515 nm at room temperature, and the data were analyzed using META-FLOUR software. Each experiment had at least 20 cells. Real-time changes in cytosolic Ca<sup>2+</sup> were displayed as a ratio of fluorescence relative to the average intensity before stimulation ( $F_t/F_0$ ).

### Xenograft experiment

Single cells were isolated from tumor spheroids in soft fibrin gel by collagenase (Sigma) and dispase II (Sigma). The cells were mixed with Matrigel (BD Biosciences) at 1:1 ratio. Xenograft procedures were similar to previous publications with modification [25, 26]. Briefly, mice were randomly assigned to either control group or experimental groups. Ketamine (80 mg/kg) and xylazine (5 mg/kg) were given to mice for anesthesia before tumor cell inoculation. Each mouse was given in one flank a subcutaneous injection of 100 μl cell/Matrigel mixture containing certain numbers of BCSC-like cells (10<sup>2</sup>, 10<sup>3</sup> or 10<sup>4</sup>) with or without Orai1 or Orai3 knock-down. Following inoculation, 100 μl of 100 μM estradiol solution (Sigma) was intraperitoneally injected to each mouse every two days and tumor growth was measured at the same days. Control and treatment mice were placed in nearby cages. Any expected and unexpected adverse event were monitored daily by a veterinarian. Tumor volume was calculated based on the formula  $V = \frac{\text{length} \times (\text{width}^2)}{2}$ . Mice were sacrificed until the diameter (width/length) of tumors reached near 2 cm and endpoint tumor weight values were measured. The tumor size was limited to no more than 2 cm in diameter to reduce animal suffering. At the experimental endpoint, mice were euthanized by CO<sub>2</sub> to minimize suffering. The number of mice used in each experimental group was 5–6, as specified in relevant Figure legends. The data from all mice were included.

### Bioinformatics

RNA-Seq data for bioinformatics analysis were sourced from The Cancer Genome Atlas (TCGA) breast cancer database and The Genotype-Tissue Expression (GTEx) database with 420 Luminal A (LumA) and 572

Normal-Like (N-Like). Normal-Like samples from TCGA and GTEx database were unified using an established database incorporation method [27].

### Patient samples and immunostaining

Human tissue experiments were approved by Ethics Committee of Affiliated Hospital of Shandong First Medical University (No. 2021001). Luminal A type breast cancer specimens along with the corresponding clinical pathologic data from 30 patients were collected from Affiliated Hospital of Shandong First Medical University (Shandong Academy of Medical Sciences) with informed consent of patients. Pathological diagnosis was performed by haematoxylin and eosin (H&E) staining and immunohistochemistry index based on PR, ER, HER2 and Ki-67. The histological grades were evaluated by Elston-Ellis modification of Scarff-Bloom-Richardson grading system which is based on the degree of duct formation, nuclear size, nuclear pleomorphism and mitotic rate [28].

For Orai1 and Orai3 immunostaining of breast samples, tissues were fixed using 10% formalin, paraffin embedded and sliced into cross-sections of 5 μm. After rehydrating in a graded alcohol series to 80% ethanol and antigen retrieval (HC ST02 Antigen Retriever—PT Module, Thermo), MXB UltraSensitive TM SP (Mice/Rabbits), IHC Kit were used to inhibit endogenous peroxidase activity and blocking. Sections were incubated at 4 °C temperature overnight with primary polyclonal antibodies to Orai1 (1:150, Proteintech) or Orai3 (1:150, Proteintech). MXB IHC Kit was consequently applied for the following immunoreactivity. The sections were then developed using DAB and the pictures were captured by microscopy (HC U02—Nikon Ni-U Eclipse Upright Microscope).

### Statistics

All data are presented as means ± SEM or mean ± SD of at least three independent experiments. Statistical analyses were performed using GraphPad Prism 8.0 software. Comparisons between two groups were measured by Student's unpaired two-tailed t-test. Differences among three or more groups were examined by one-way analysis of variance (ANOVA) test followed by Tukey's multiple comparisons test. Comparisons among multiple growth curves of tumors or tumor spheroids were performed by two-way ANOVA followed by Bonferroni post-test. *P* value < 0.05 was considered as significantly different. Conclusions would not be drawn if relevant comparisons could not reach statistical significance.

**Results**

**Orai1 promotes the growth of tumor spheroids and increases cancer cell stemness in vitro**

3D soft fibrin gel was used to enrich BCSC-like cells from ER+ breast cancer cells MCF7 and MDA-MB-415 using the method described elsewhere [16]. MCF7 and

MDA-MB-415 cells were seeded in 90 Pa soft fibrin gel. Within a few days, they grew to form tumor spheroids [16]. Western blot showed that the 3D gel-enriched BCSC-like cells in tumor spheroids had a substantially higher expression of Orai1 than that of 2D cultured ordinary cancer cells (Fig. 1A, S1A). Three lentiviral-based

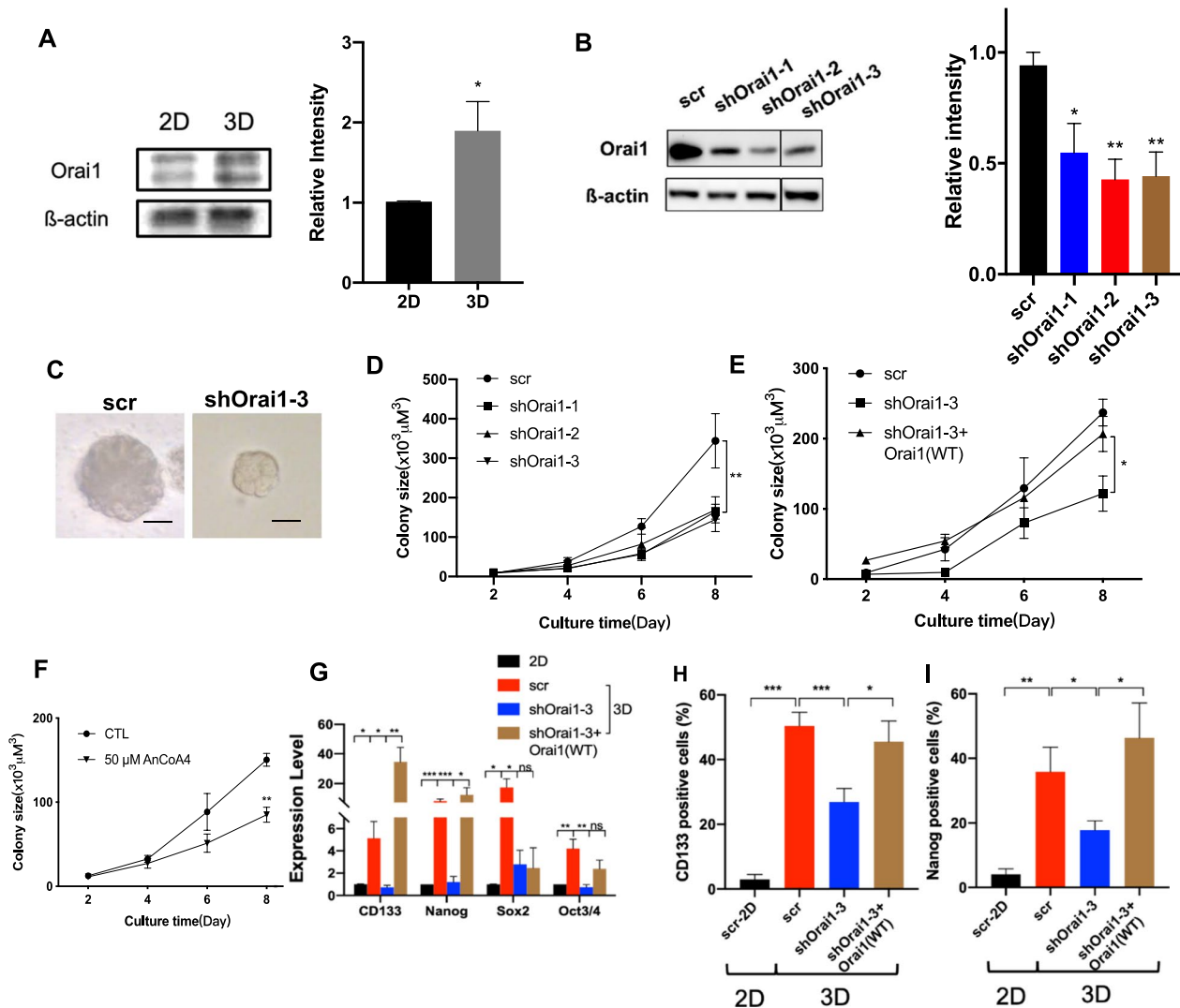


**Fig. 1** Orai1 promotes the growth of tumor spheroids and increases stemness of MCF7 BCSC-like cells. **A** The protein expression of Orai1 in MCF7 cells grown in 2D culture or in 3D 90 Pa soft fibrin gel with representative western blot images (left) and summary data normalized to  $\beta$ -actin (right) (n=4). **B** The protein expression of Orai1 in MCF7 cells treated with lenti-scrambled-shRNA or lenti-Orai1-shRNAs. Shown are representative western blot images (left) and summary data normalized to  $\beta$ -actin (right) (n=4). **C** and **D** The growth of tumor spheroids (colonies) formed by MCF7 cells in 3D 90 Pa soft fibrin gel with or without Orai1 knockdown, shown photographically (**C**) and graphically (**D**). Bar, 50  $\mu$ m (n=4–10). **E** Orai1 overexpressing plasmid was re-introduced to the Orai1 knockdown MCF7 cells. Shown was the growth of MCF7 tumor spheroids with lenti-scrambled-shRNA or lenti-Orai1-shRNA or lenti-Orai1-shRNA + Orai1 plasmid (n=4). **F** MCF7 cells were pre-treated with Orai1 inhibitor (AnCoA4, 50  $\mu$ M) for two days before seeded in 90 Pa fibrin gel for spheroid growth. AnCoA4 was maintained in the culture medium. DMSO was used as control. The spheroid size was shown graphically (n=4). **G** RT-qPCR analysis of cancer stem cell markers in MCF7 cells, showing the effect of 3D culture, lenti-Orai1-shRNA, and lenti-Orai1-shRNA plus Orai1 plasmid (n=4–8). **H** and **I** Summary of flow cytometric results showing the percentage of CD133-positive (**H**, n=5–12) and Nanog-positive (**I**, n=5–11) cells. The cells were treated with lenti-scrambled-shRNA or lenti-Orai1-shRNA or lenti-Orai1-shRNA plus Orai1 plasmid. Mean  $\pm$  SEM. ns, not significant; \*,  $P < 0.05$ ; \*\*,  $P < 0.01$ ; \*\*\*,  $P < 0.001$ , by Student t test in **A**, or one-way ANOVA in **B** and **G–I** or two-way ANOVA in **D–F**. Original western blot images are provided as Additional File #2.

Orai1-shRNAs were constructed, all of which could effectively knockdown the expression of Orai1 in MCF7 cells by western blots (Fig. 1B) and RT-qPCRs (Fig. S2A). RT-qPCRs further confirmed that overexpression of exogenous Orai1 could reverse the knockdown effect of Orai1-shRNAs, significantly increasing Orai1 expression (Fig. S2B). Similar results were obtained using Orai1-siRNA in MDA-MB-415 cells (S1B, S2C–D).

A key feature of BCSCs is self-renewal capacity, which is the driving force of tumorigenic initiation [29]. Growth kinetics of tumor spheroids is an indicator of BCSC renewal capacity. Interestingly, Orai1 RNA silencing reduced the growth of BCSC-like cells in tumor spheroids (Fig. 1C–D, S1C–D), the effect of which could be rescued by overexpression of exogenous Orai1 (Fig. 1E, S1D). An Orai1 inhibitor AnCoA4 at 50  $\mu$ M [30] also inhibited the growth of BCSC-like cells in tumor spheroids (Fig. 1F, S1E). However, Orai1 RNA silencing had no effect on the growth of 2D cultured cancer cells (Figs. S3A, S3C), suggesting that Orai1 knockdown preferentially inhibited the growth of BCSC-like cells in tumor spheroids but not that of ordinary breast cancer cells (non-CSCs) grown in conventional 2D culture.

Importantly, the cells in tumor spheroids were CSC-like, displaying higher expression levels of multiple CSC markers (Fig. 1G, S1F) and showing higher chemoresistance than 2D cultured cells (Fig. S2E, F). Based on flow cytometer analysis of BCSC markers (CD133 and Nanog for MCF7, CD133 and CD44 for MDA-MB-415), 3D tumor spheroids contained about 34–70% BCSCs, whereas 2D cultured cells only contained 3–5% BCSCs (Fig. 1H–I, S1G–H). Importantly, RT-qPCR showed that Orai1 RNA silencing reduced the expression levels of multiple BCSC markers (CD133, Nanog, Sox2, and Oct3/4) (Fig. 1G, S1F), whereas overexpression of exogenous Orai1 reversed the effect of Orai1 RNA silencing and elevated the expression of several BCSC markers (Fig. 1G, S1F). Flow cytometry analysis further confirmed that Orai1 RNA silencing reduced the expression of CD133 and Nanog/CD44, the effect of which was reversed by overexpression of exogenous Orai1 (Fig. 1H–I, S1G–H).

### Orai1 promotes tumorigenicity in vivo

A gold standard method of studying CSCs is to determine their capability of tumor formation in NOD/SCID mice.

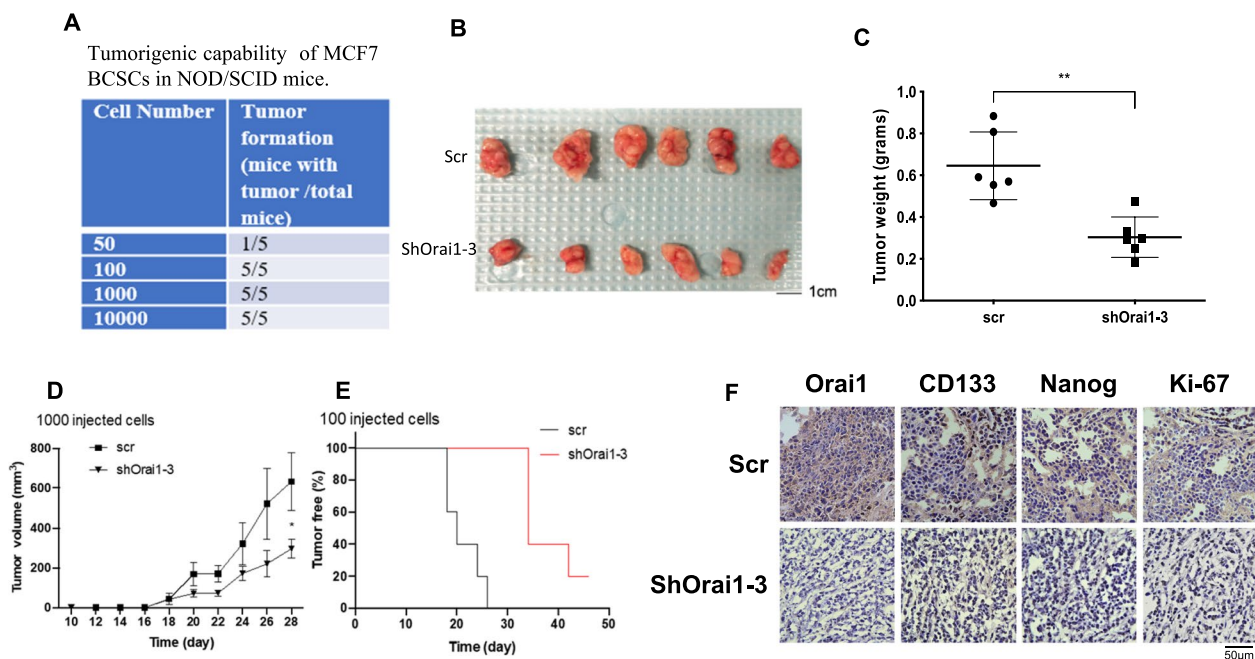


**Fig. 2** Orai1 promotes tumorigenicity of MCF7 BCSC-like cells in NOD/SCID mice. **A** Tumorigenic capability of MCF7 BCSC-like cells derived from 3D fibrin gel tumor spheroids in NOD/SCID mice ( $n = 5$ ). **B** and **C** The mice were injected with MCF7 BCSC-like cells carrying lenti-scrambled shRNA or lenti-Orai1-shRNA ( $n = 6$ ). Shown are images of endpoint primary tumor size (**B**) and summary of endpoint tumor weight (**C**) in NOD/SCID mice. Bar, 1 cm. **D** Tumor growth curve in NOD/SCID mice injected with 1000 BCSC-like cells carrying lenti-scrambled shRNA or lenti-Orai1-shRNA over 28 days post injection ( $n = 5$ ). **E** Tumor incidence in NOD/SCID mice injected with 100 MCF7 BCSC-like cells carrying lenti-scrambled shRNA or lenti-Orai1-shRNA ( $n = 5$ ). **F** Immunohistochemical analysis of expression of Orai1, CD133, Nanog and Ki67 in primary tumors with lenti-scrambled shRNA or lenti-Orai1-shRNA ( $n = 3$ ). A total of 52 mice were used for experiments in this Figure. Bar, 50  $\mu$ m. Mean  $\pm$  SD. \*,  $P < 0.05$ ; \*\*,  $P < 0.01$ , by Student *t* test in B, or two-way ANOVA in D

We isolated BCSC-like cells from 3D MCF7 tumor spheroids. Subcutaneously injection of only 100 such BCSC-like cells to NOD/SCID mice could successfully induce tumor formation in all mice (5 out of 5 mice) (Fig. 2A), indicating remarkable tumorigenic capability of these BCSC-like cells. Note that MCF7 cells are low aggressive cancer cells. A few millions of MCF7 cells are often needed to be injected for tumor formation in NOD/SCID mice [31]. Therefore, our 3D soft fibrin gel platform is highly robust in enriching tumorigenic cells.

Importantly, Orai1 RNA silencing with lenti-Orai1-shRNA reduced tumor xenograft growth in NOD/SCID mice, with smaller endpoint tumor size (Fig. 2B) and less endpoint tumor weight on day 30 after injection (Fig. 2C), and slower tumor growth rate (Fig. 2D). Orai1 RNA silencing also prolonged tumor free duration (Fig. 2E). Immunostaining on tumor sections confirmed that lenti-Orai1-shRNA could effectively knockdown the expression of Orai1 and reduce the expression of CD133, Nanog and Ki-67 in xenograft tumors (Fig. 2F).

### Orai1 stimulates glycolysis pathway

We examined the metabolic profile of 3D gel-enriched BCSC-like cells. RNA seq experiments followed by KEGG pathway enrichment analysis demonstrated that glycolysis was the most significantly upregulated pathway in 3D gel-enriched BCSC-like cells compared with 2D cultured cells (Fig. 3A). RT-qPCR analysis confirmed that 3D culture indeed caused upregulation of multiple glycolytic genes (Fig. 3B, S4A). Furthermore, a glycolysis inhibitor 2-DG at 5 mM dramatically suppressed the growth of tumor spheroids (Fig. 3C, S4B), suggesting that glycolysis is a key player in BCSC growth.

Interestingly, Orai1 inhibitor AnCoA4 at 50  $\mu$ M or Orai1 RNA silencing decreased the expression of multiple glycolytic genes in 3D gel-enriched BCSC-like cells (Fig. 3D–E, S4C–D). Orai1 RNA silencing also reduced glucose uptake, pyruvate level and lactate production in 3D gel-enriched BCSC-like cells (Fig. 3F–H). However, Orai1 RNA silencing did not affect the expression of glycolytic genes in 2D cultured cells (Fig. 3E, S4D).

Together, these results identified a novel function of Orai1 in regulating glycolysis pathway in BCSCs.

### Orai1 mediates SICE whereas Orai3 mediates SOCE

It was previously reported that in ER+breast cancer cells, Orai1-SPCA2 mediates SICE whereas Orai3-STIM1 mediates SOCE [6, 7]. Indeed, we found that in MCF7 cells and MDA-MB-415 cells, small molecule inhibitors of Orai1 AnCoA4 and RO2959 (Figs. S5A–B, S6A–B), and Orai1 RNA silencing (Figs. S5C–D, S6A–B) all reduced the basal  $Ca^{2+}$  influx (or SICE) initiated by  $Ca^{2+}$  addback to the bath. In contrast, Orai3 RNA silencing had no effect on SICE (Figs. S5D, S6A–B). We also studied SOCE and found that Orai1 RNA silencing did not alter the SOCE (Figs. S5E–F, S6C–D), whereas RNA silencing of Orai3 or STIM1 substantially reduced the SOCE (Figs. S5G–I, S6C, E, F). These data support the notion that Orai1 mediates SICE while Orai3 mediates SOCE in ER+breast cancer cells as reported by others [6, 7].

### Orai1 interacts with SPCA2 to mediate SICE and promote glycolysis

It was reported that Orai1 interacts with SPCA2 to mediate SICE [7, 32]. Two lentiviral-based SPCA2-specific shRNAs were constructed, each of which could effectively knockdown the expression of SPCA2 in western blots in MCF7 cells (Fig. 4A). As expected, knockdown of SPCA2 reduced the SICE (Fig. S7A–B,D). Similar results were obtained using SPCA2-siRNA in MDA-MB-415 cells (S6A–B). To demonstrate the functional role of Orai1-SPCA2 physical interaction, we employed an N-terminal fragment of SPCA2 (SPCA2-N), which was previously reported to interfere the interaction of SPCA2 with Orai1, consequently exerting dominant negative effect on Orai1-SPCA2-mediated SICE [7, 32]. Indeed, we found that SPCA2-N could reduce the SICE (Figs. S7C–D, S6A–B). Furthermore, SPCA2-N and/or SPCA2-shRNA reduced the growth of tumor spheroids (Fig. 4B, S8A) and downregulated the expression of glycolytic genes except ENO2 and ALDOA in MCF7 BCSC-like cells (Fig. 4C–D, S8B).

(See figure on next page.)

**Fig. 3** Orai1 stimulates glycolysis pathway in MCF7 BCSC-like cells. **A** and **B** Shown were the KEGG pathway enrichment analysis of upregulated genes (**A**) in 3D 90 Pa soft fibrin gel-enriched MCF7 BCSC-like cells compared to 2D cultured MCF7 cells, and confirmation of glycolysis pathway by RT-qPCR (**B**,  $n=3$ ). **C** The growth of MCF7 tumor spheroids (colonies) in 3D soft fibrin gel treated with or without glycolysis inhibitor, 2-DG, over 8 days ( $n=3$ ). **D** Relative fold change of glycolytic genes in 3D gel-enriched MCF7 BCSC-like cells treated with or without 50  $\mu$ M AnCoA4, as detected by RT-qPCR. The data were normalized to  $\beta$ -actin ( $n=3$ ). **E** Relative fold change of glycolytic genes in 3D gel-enriched MCF7 BCSC-like cells and 2D cultured MCF7 cells with or without Orai1 knockdown as detected by RT-qPCR ( $n=3-5$ ). **F** Glucose uptake shown as mean fluorescent intensity (MFI) of 2-NBDG in 3D gel-enriched MCF7 BCSC-like cells with or without Orai1 knockdown ( $n=5$ ). **G** and **H** Relative fold change of pyruvate production (**G**) and lactate levels (**H**) in 3D gel-enriched MCF7 BCSC-like cells with or without Orai1 knockdown ( $n=5$ ), Mean  $\pm$  SEM. ns, not significant; \*,  $P < 0.05$ ; \*\*,  $P < 0.01$ ; \*\*\*,  $P < 0.001$ , by Student t test in **B**, **D**, **F**, **G** and **H**, or two-way ANOVA in **C** and **E**

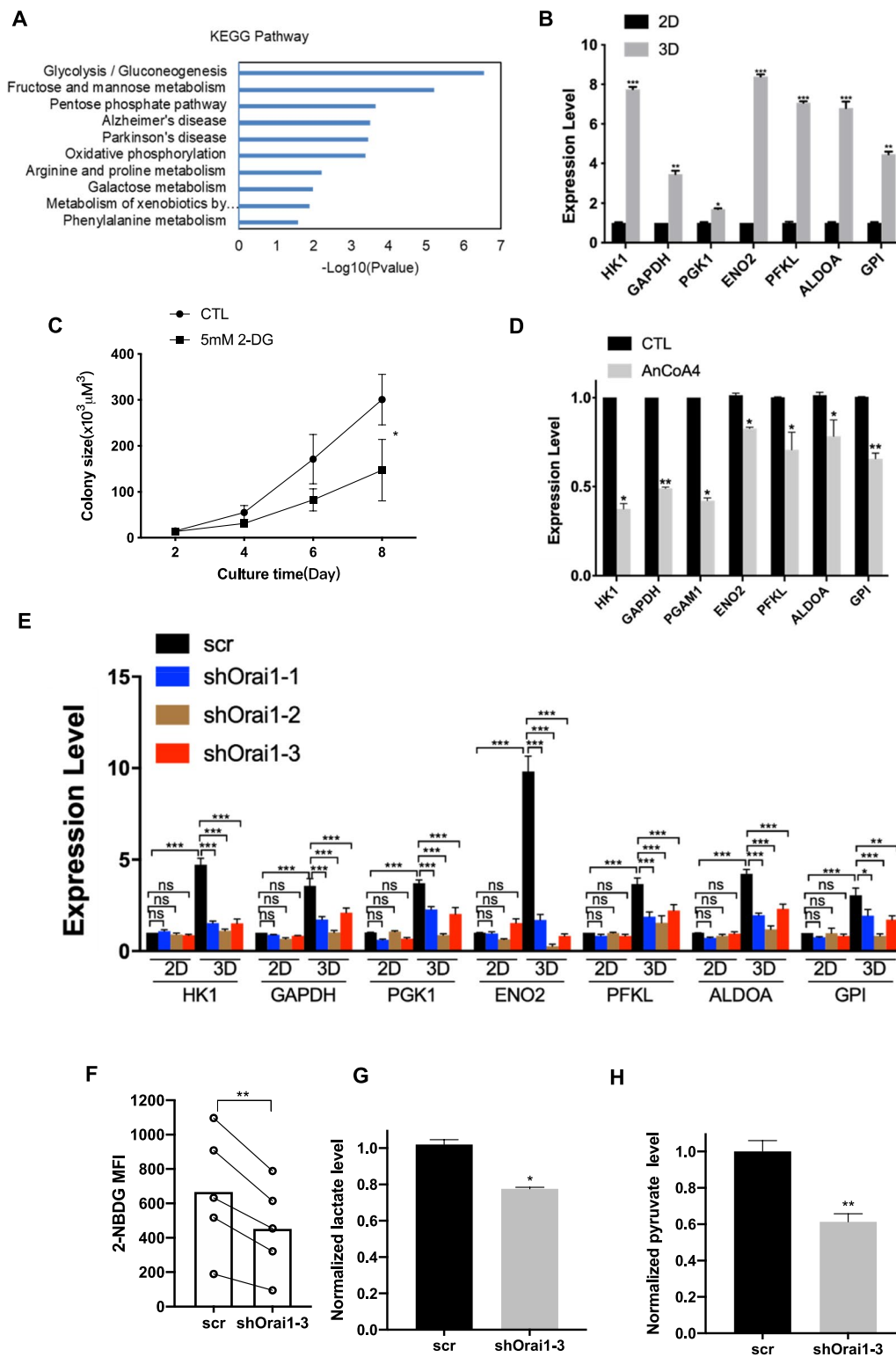


**Fig. 3** (See legend on previous page.)



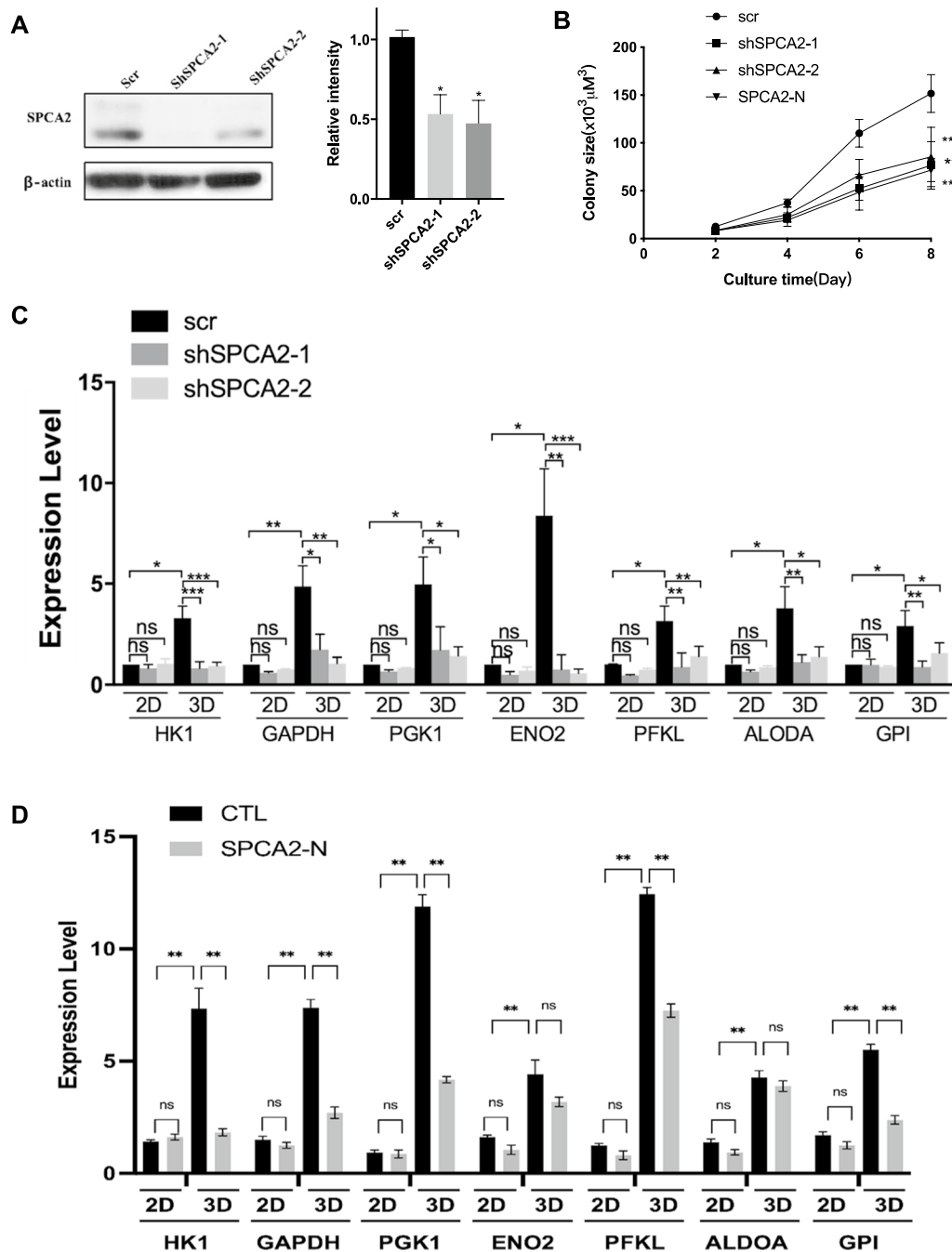


**Fig. 4** SPCA2 interacts with Orai1 to promote glycolysis in MCF7 BCSC-like cells. **A** Western blot analysis showing the expression of SPCA2 in MCF7 cells transfected with lenti-scrambled-shRNA or lenti-SPCA2-shRNAs (n=3). **B** The growth of tumor spheroids (colonies) formed by MCF7 cells in 3D 90 Pa soft fibrin gel with or without SPCA2 knockdown or addition of SPCA2 N-terminal fragment (n=4–6). **C–D** Relative fold change of glycolytic genes in MCF7 cells with or without SPCA2 knockdown (**C**) or with or without addition of SPCA2 N-terminal fragment (**D**) as detected by RT-qPCR. The results from both 2D cultured and 3D cultured MCF7 cells were shown (n=3–5). Mean ± SEM. ns, not significant; \*, P < 0.05, \*\*, P < 0.01, \*\*\*, P < 0.001, by one-way ANOVA in **B**, or two-way ANOVA in **C–D**. Original western blot images are provided as Additional File #2

### Orai3 and STIM1 promote the growth of tumor spheroids and increases cancer cell stemness in vitro, and tumorigenicity in vivo

We next explored the role of Orai3 and STIM1 in the growth of tumor spheroids. Western blot analysis

showed that the 3D gel-enriched BCSC-like cells had a substantially higher expression of Orai3 than that in 2D cultured cells (Fig. 5A, Fig. S9A). Lentiviral-based Orai3-shRNAs and STIM1-shRNAs were constructed, all of which could knockdown the expression of their

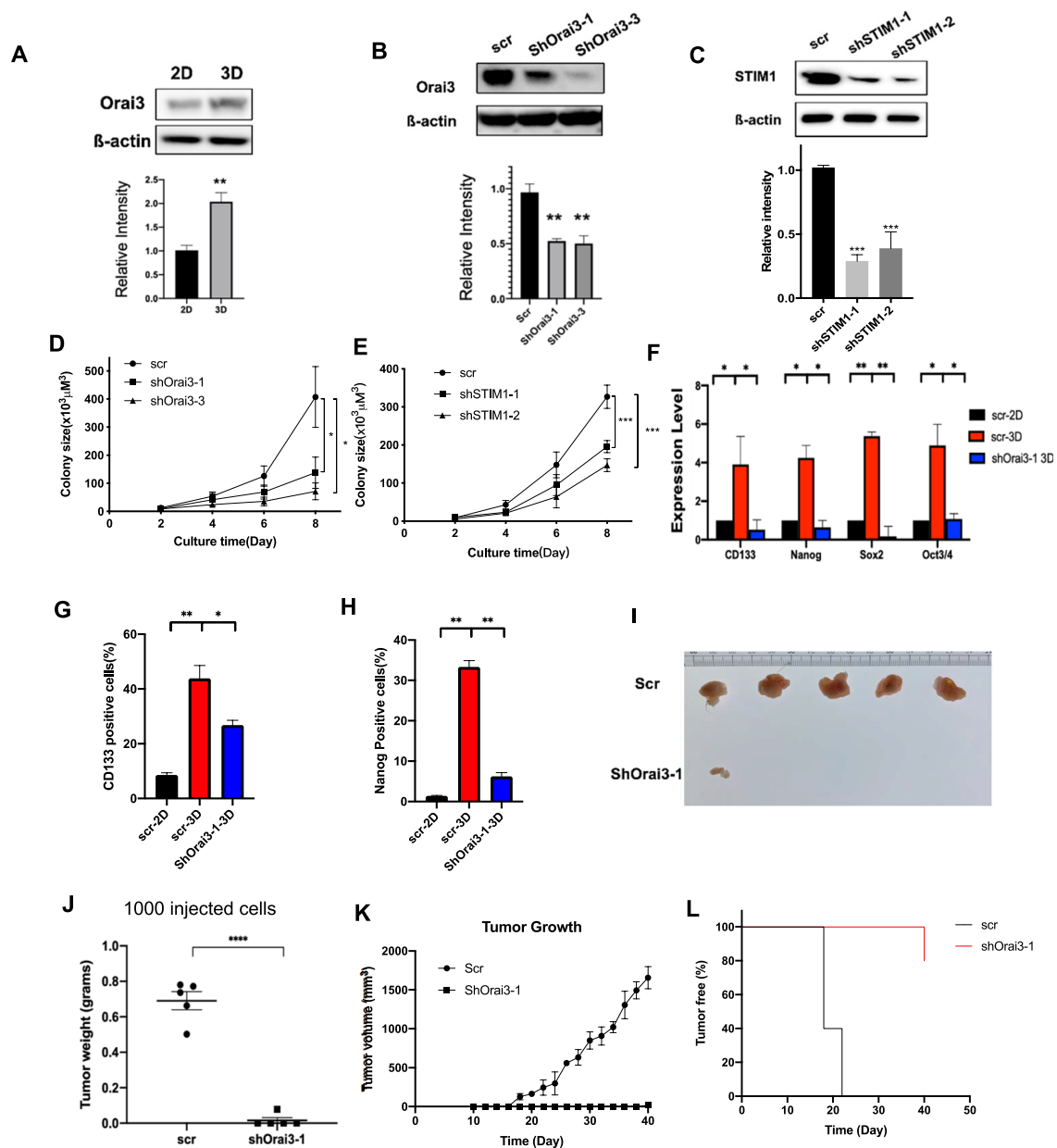


**Fig. 5** Orai3 promotes the growth of tumor spheroids in vitro and tumorigenicity of MCF7 BCSC-like cells in vivo. **A** The protein expression of Orai3 in MCF7 cells grown in 2D culture or in 3D 90 Pa soft fibrin gel with representative western blot images (up) and summary data normalized to  $\beta$ -actin (bottom) ( $n=3$ ). **B** and **C** Representative western blot images and summary data showing the expression of Orai3 (**B**) and STIM1 (**C**) in MCF7 cells transfected with lenti-scrambled-shRNA or lenti-Orai3-shRNA or lenti-STIM1-shRNA ( $n=3$ ). **D** and **E** The growth of tumor spheroids formed by MCF7 cells in 3D 90 Pa fibrin gel with or without Orai3 knockdown (**D**) or STIM1 knockdown (**E**) ( $n=4$ ). **F** RT-qPCR analysis of cancer stemness markers in MCF7 cells, showing the effect of 3D culture and lenti-Orai3-shRNA ( $n=4$ ). **G** and **H** Summary of flow cytometric results showing the effect of 3D culture and lenti-Orai3-shRNA on the percentage of CD133-positive (**G**,  $n=5$ ) and Nanog-positive (**H**,  $n=5$ ) cells. **I–L** Tumorigenic capability of BCSC-like cells in NOD/SCID mice. The mice were injected with BCSC-like cells carrying lenti-scrambled-shRNA or lenti-Orai3-shRNA ( $n=5$ ). Shown are images of endpoint primary tumor size (**I**) and summary of endpoint tumor weight (**J**) in NOD/SCID mice. Bar, 1 cm. **K** Tumor growth curve in NOD/SCID mice injected with  $10^3$  BCSC-like cells carrying lenti-scrambled-shRNA or lenti-Orai3-shRNA over 40 days post injection ( $n=5$ ). **L** Tumor incidence in NOD/SCID mice injected with  $10^3$  MCF7 BCSC-like cells carrying lenti-scrambled-shRNA or lenti-Orai3-shRNA ( $n=5$ ). A total of 20 mice were used for experiments in this Figure. Mean  $\pm$  SEM. \*,  $P < 0.05$ ; \*\*,  $P < 0.01$ ; \*\*\*,  $P < 0.001$ ; \*\*\*\*,  $P < 0.0001$ , by Student  $t$  test in **A** and **J**, one way ANOVA in **B**, **C**, **F–H**, or two-way ANOVA in **D**, **E** and **K**. Original western blot images are provided as Additional File #2

respective targets in MCF7 cells (Fig. 5B–C). Orai3-siRNA also had similar knockdown effect in MDA-MB-415 cells (Fig. S9B). Importantly, RNA silencing of Orai3 and STIM1 each reduced the growth of tumor spheroids (Fig. 5D–E, Fig. S9C). Furthermore, RT-qPCR analysis showed that Orai3 RNA silencing reduced the expression levels of several BCSC markers in BCSC-like cells (Fig. 5F, Fig. S9D). Flow cytometry analysis further validated that Orai3 RNA silencing reduced the expression of CD133 and Nanog/CD44 (Fig. 5G–H, Fig. S9E). These data strongly suggest that Orai3 promotes stemness of BCSC-like cells. Interestingly, knockdown of Orai3 had minimal effect on the growth of 2D cultured cells (Fig. S3B, D), suggesting that Orai3 knockdown preferentially inhibited the growth of BCSC-like cells in tumor spheroids but not that of ordinary breast cancer cells (non-CSCs) grown in conventional 2D culture.

Importantly, lenti-Orai3-shRNA nearly abolished tumor xenograft growth in NOD/SCID mice. In control,

all 5 mice grew tumors 40 days after injection with 1000 of BCSC-like cells derived from 3D MCF7 tumor spheroids. In contrast, with lenti-Orai3-shRNA, only 1 out of 5 mice grew a small-sized tumor (51) with summarized data in Fig. 5J–L. These results support the importance of Orai3 in stemness, self-renewal and tumorigenicity of BCSC-like cells.

#### Knockdown of Orai3 and STIM1 does not affect glycolysis pathway

RT-qPCR was conducted to determine the effect of Orai3 and STIM1 knockdown on the expression of glycolytic genes in BCSC-like cells. The results showed that RNA silencing of Orai3 (Fig. 6A, Fig. S9F) and STIM1 (Fig. 6B) had no effect on the expression of multiple glycolytic genes. These data suggest that Orai3 and STIM1 promotes the self-renewal of BCSC-like cells through a mechanism independent of glycolysis pathway.

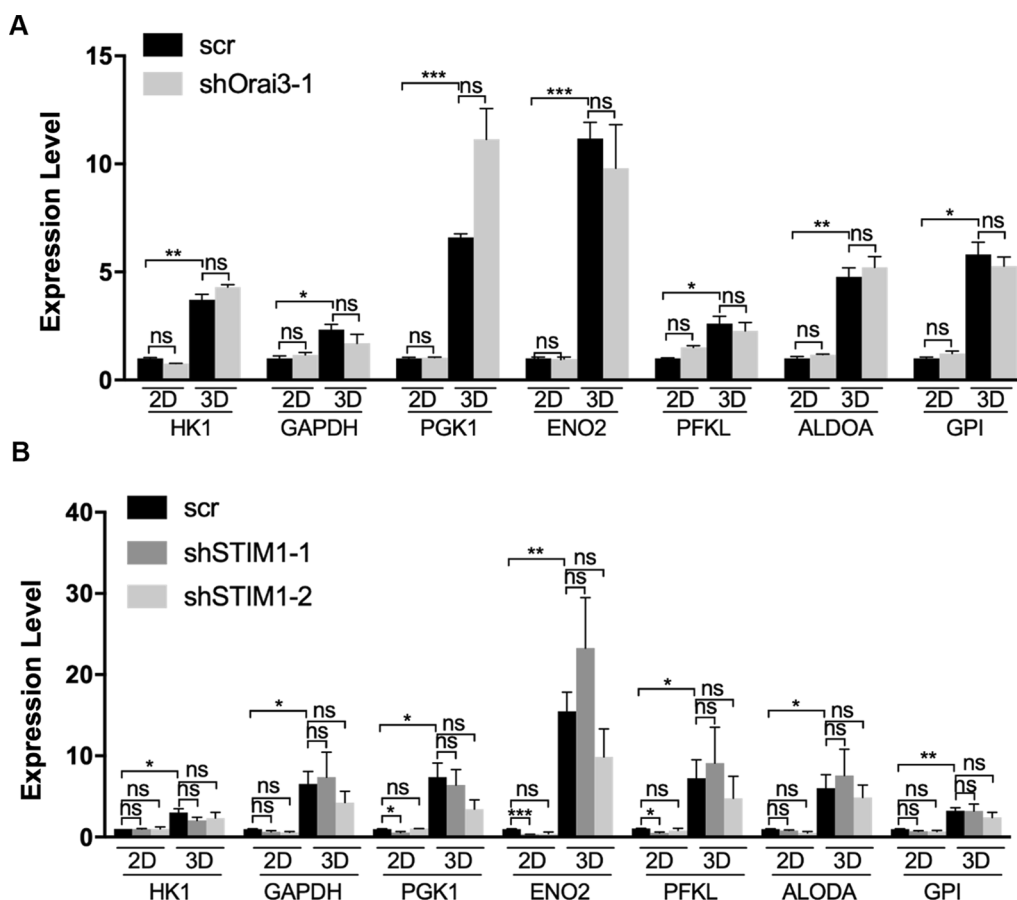


**Fig. 6** Orai3 and STIM1 do not affect glycolysis in MCF7 BCSC-like cells. Shown are relative fold change of glycolytic genes in MCF7 cells with or without Orai3 knockdown (A) or STIM1 knockdown (B). The results from both 2D cultured and 3D cultured MCF7 cells were shown. Mean ± SEM. ns, not significant; \*,  $P < 0.05$ , \*\*,  $P < 0.01$ , \*\*\*,  $P < 0.001$ , by two-way ANOVA

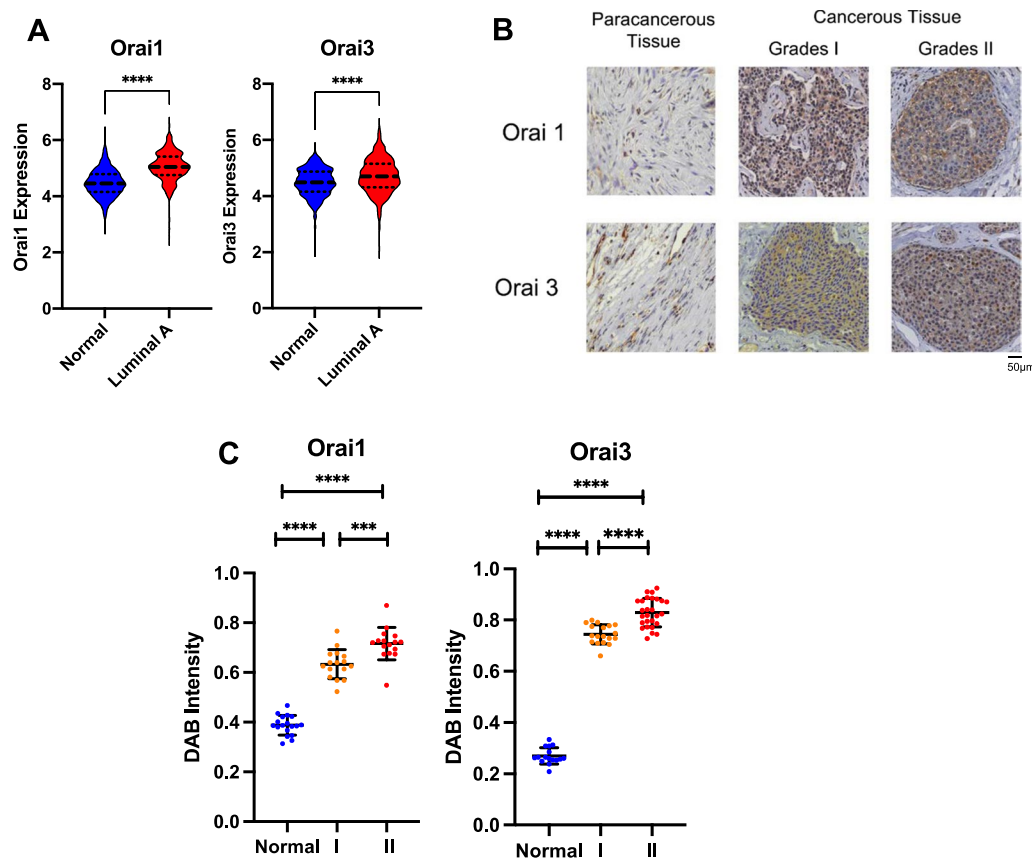


**Fig. 7** Expression of Orai1 and Orai3 is elevated in the tumor samples of luminal A breast cancer. **A** Expression analysis of Orai1 and Orai3 in luminal A breast tumors and normal breast tissues from The Cancer Genome Atlas (TCGA) cohort plus GTEx database. **B** Representative immunohistochemical staining images comparing the expression of Orai1 and Orai3 between normal tissue and patients' samples with different histological grades of luminal A breast cancer. Bar, 50 µm. **C** Quantitative analysis of Orai1 and Orai3 expression levels as in **B**, with each dot representing the sample from one patient. Mean  $\pm$  SD. \*\*\*\*,  $P < 0.0001$ , by Student *t* test in **A** and one way ANOVA in **C**

#### Expression levels of Orai1 and Orai3 are elevated in the tumor tissues of luminal A type breast cancer

To explore the clinical relevance of Orai1 and Orai3 in human luminal A type breast cancer, meta-analysis was performed in RNAseq datasets in TCGA breast cancer database plus GTEx database. The results showed that the expression levels of both Orai1 and Orai3 are significantly upregulated in the breast tissues of luminal A breast cancer compared with normal tissues (Fig. 7A). We further analysed the expression levels of Orai1 and Orai3 proteins in tumor sections of 30 luminal A type breast cancer patients. The results revealed an increased expression levels of Orai1 and Orai3 in human breast cancer tissues compared with normal breast tissues in a tumor histological grade-dependent manner (Fig. 7B and C).

#### Discussion

One of major challenges in breast tumor therapy is the existence of BCSCs, which are resistant to current therapies. This is partly due to our insufficient knowledge

about the physiology of BCSCs. Up to now, there is only very limited research on the role of  $Ca^{2+}$  signaling in BCSCs. In one study, Lu et al. [33], demonstrated an important role of RYR1, an endoplasmic reticulum  $Ca^{2+}$  releasing channel, in the BCSC enrichment. In another study, Hirata et al. [34], showed that lysophosphatidic acid can promote the expansion of BCSCs via a  $Ca^{2+}$  entry channel TRPC3. With regard to Orai channels, recent studies have reported the role of Orai1 and Orai3 in CSCs of glioblastoma, non-small cell lung cancer and oral/oropharyngeal squamous cell carcinoma [35–38]. However, none of these previous studies have investigated Orai1 or Orai3 in the context of BCSCs. In the present study, we explored the role of Orai1 and Orai3 in the BCSC-like cells enriched from ER+ breast cancer cells using 3D soft fibrin gel. The expression levels of Orai1 and Orai3 were found to be elevated in these BCSC-like cells as well as in tissue samples from luminal A breast cancer patients. Knockdown of Orai1 and Orai3 reduced the growth of tumor spheroids

in 3D soft fibrin gel and decreased the expression of BCSC markers. More importantly, after knockdown of either Orai1 or Orai3, tumorigenic ability of BCSC-like cells in NOD/SCID mice were markedly reduced, with reduced tumor growth and prolonged tumor free duration. These data provide strong evidence for a crucial role of Orai1 and Orai3 in self-renewal and tumorigenicity of BCSCs.

Metabolic phenotype is a crucial determinant of BCSC properties [12, 13]. Compared with the differentiated breast cancer cells, BCSCs strongly favor the glycolysis pathway, which allows BCSCs to obtain energy faster than oxidative phosphorylation pathway [12, 14, 39]. Indeed, we found that top 3 upregulated gene categories in KEGG analysis between 3D cultured BCSCs and 2D cultured ordinary cancer cells are all related to the metabolic pathway of hexose and pentose, suggesting a huge change in energy acquisition pathway genes when cells switch from 2D-culture to 3D-culture. Furthermore, RT-qPCR analysis found that the basal expression of glycolytic genes is also much higher in 3D cultured BCSCs compared with 2D cultured ordinary cancer cells, confirming a switch of metabolic pathway to more active glycolysis in 3D cultured BCSCs. Moreover, a glycolysis inhibitor 2-DG substantially suppressed the growth of 3D tumor spheroids. These data demonstrate a critical role of glycolysis in the growth of BCSC-like cells.

Ca<sup>2+</sup> is a versatile signal that regulates diverse cellular processes in cancer [40]. Store-operated Ca<sup>2+</sup> entry is reported to regulate glycolysis in T lymphocytes [41]. Recently, another Ca<sup>2+</sup>-permeable channel TRPM7 is reported to regulate glycolytic reprogramming in ordinary colorectal cancer cells and breast cancer cells [42]. However, up to the present, virtually nothing is known about Ca<sup>2+</sup> regulation of glycolysis pathway in cancer stem cells. In our study, Orai1 expression was found to be upregulated in 3D gel-enriched BCSC-like cells compared with 2D cultured breast cancer cells, which correlated with an upregulation of glycolytic pathway in 3D gel-enriched BCSC-like cells. RNA silencing of Orai1 or SPCA2, or pharmacological inhibition of Orai1 substantially downregulated the expression of glycolytic genes in BCSC-like cells. Orai1 knockdown also reduced glucose uptake, pyruvate level and lactate production in 3D gel-enriched BCSC-like cells, all of which are glycolysis-related indexes. These data established a clear functional linkage between Orai1-SPCA2 and the Warburg effect (glycolysis) in BCSCs. In this regard, others have reports that hypoxic tumor microenvironment in 3D tumor spheroids may cause upregulation of Orai1 expression, at least in colon cancer cells [43]. Therefore, a likely scenario is that hypoxic microenvironment in 3D tumor spheroids

may stimulate Orai1 expression in BCSCs, causing consequent increase in Ca<sup>2+</sup> entry via Orai1-SPCA2, which in turn stimulates the glycolysis pathway to promote self-renewal and tumorigenicity of these BCSCs. Herein, our data for the first time establish a mechanistic linkage between two important signalling pathways, namely Orai1-mediated Ca<sup>2+</sup> signalling and glycolysis, in BCSC function.

In ER+ breast cancer cells, it has been reported that Orai1-SPCA2 mediates SICE whereas Orai3-STIM1 mediates SOCE [6, 7], which was confirmed by this study (Figs. S5–S6). Intriguingly, our present study demonstrated that Orai1-SPCA2 and Orai3-STIM1 act through two distinct downstream signaling axes to regulate self-renewal and tumorigenicity of BCSCs. Herein, Orai1-SPCA2 mediates SICE to activate glycolysis pathway, whereas Orai3 and STIM1 mediates SOCE to activate a glycolysis-independent pathway, both of which subsequently regulate the self-renewal and tumorigenicity of BCSC-like cells. This novel scheme illustrates an elegant regulatory mechanism through which Orai1 and Orai3 act through distinct signaling axes to finely control the self-renewal and tumorigenicity of BCSCs. An overall scheme is depicted Fig. 8.

An emerging strategy in breast cancer therapy is to target BCSC metabolism, including glycolysis pathway, in order to eliminate BCSCs [12, 13]. In the present study, we uncovered Orai1-SPCA2-SICE as an upstream signal to regulate glycolysis. These results highlight an intriguing possibility of targeting Orai1-SPCA2-glycolysis pathway as a novel strategy to eliminate BCSCs. However, literature also showed that due to their metabolic flexibility, BCSCs can switch between oxidative phosphorylation and glycolysis [12]. Thus, targeting a single metabolic pathway may not always be sufficient for complete eradication of breast tumors. Dual inhibition of glycolytic and oxidative pathways might be more effective in breast cancer therapy [12, 13]. Indeed, we found that silencing of Orai3 and STIM1, which mediates SOCE, could also markedly reduce the growth of BCSC-like cells in a glycolysis-independent manner. Therefore, we speculate that dual inhibition of Orai1-SPCA2 and Orai3-STIM1 may have a stronger inhibition on (or totally abolish) the growth and tumorigenicity of BCSCs.

Note that, the BCSCs in the present study were derived from MCF7 and MDA-MB-415 cells, both of which belong to luminal A ER+ breast cancer [44]. In clinical practice, luminal A breast cancer is often treated with endocrine therapy. However, some patients with luminal A breast cancer develop resistance to endocrine therapy due to existence of BCSCs [45]. Furthermore, one characteristic of luminal A breast cancer is the long duration of cancer recurrence up to 20 years, which is at least partly

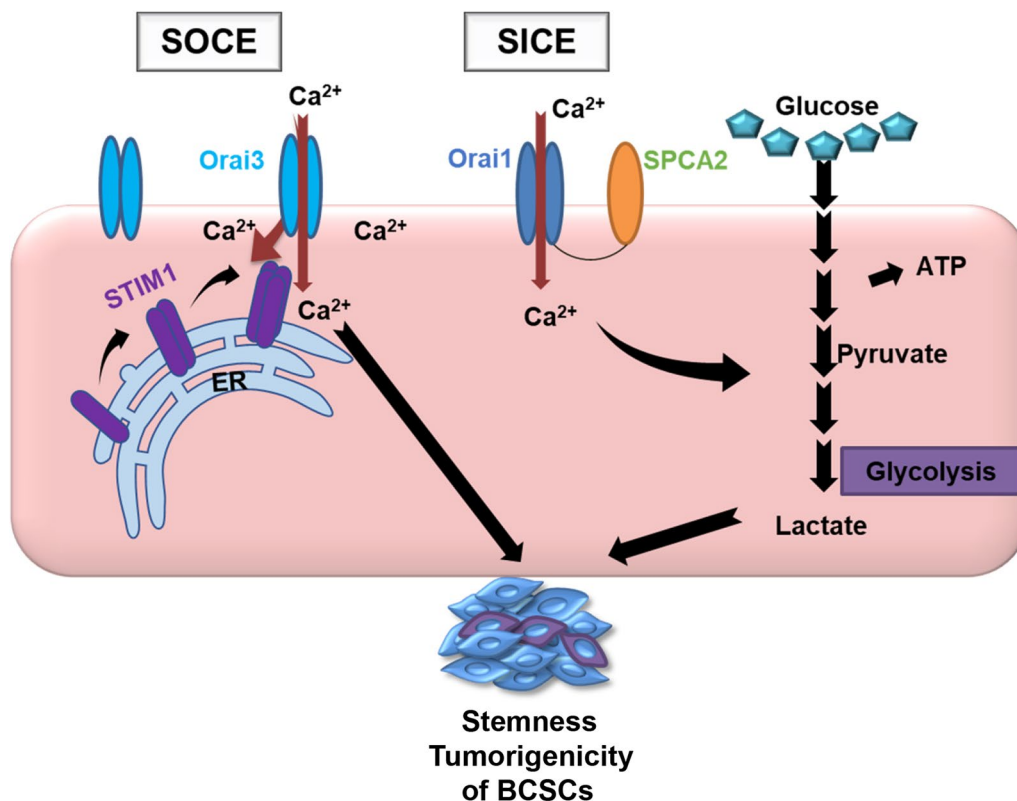


**Fig. 8** Schematic illustration of Orail-SPCA2 and Orail3-STIM1 regulation on the stemness and tumorigenicity of BCSCs. Orail1 interacts with SPCA2 to mediate SICE, which activates glycolytic pathway to promote stemness and tumorigenic ability of BCSCs. On the other hand, Orail3 and STIM1 mediate SOCE, which promotes stemness and tumorigenic ability of breast cancer cells via a glycolysis-independent mechanism

due to the existence of BCSCs [46]. Therefore, our current findings about the role of Orail in BCSCs are more relevant to luminal A breast cancer. Further studies are needed to determine whether similar mechanisms also exist in other types of breast cancer.

In conclusion, the present study demonstrated that Orail1 interacts with SPCA2 to mediate SICE, subsequently promoting the growth and tumorigenicity of BCSC-like cells via glycolysis pathway. In contrast, Orail3 and STIM1 mediate SOCE, consequently promoting the growth and tumorigenicity of BCSC-like cells via a glycolysis-independent pathway. In future, it is worth to explore therapeutic potential of targeting these pathways in breast cancer treatment.

#### Abbreviations

BCSCs	Breast cancer stem cells
Calcium-free PSS	Calcium-free physiological saline solution
CPA	Cyclopiazonic acid
CSCs	Cancer stem cells
2-DG	2-Deoxy-D-glucose
ER+	Estrogen receptor-positive
FBS	Fetal bovine serum
GTEX	The genotype-tissue expression database
5-fu	5-Fluorouracil

HEK293	Human embryonic kidney 293 cell line
2-NBDG	2-(N-Nitrobenz-2-oxa-1,3-diazol-4-yl)amino
PS	Penicillin-streptomycin
RT-qPCR	Reverse transcription-quantitative polymerase chain reaction
SICE	Store-independent $Ca^{2+}$ influx
SOCE	Store-operated $Ca^{2+}$ entry
SPCA2	The secretory pathway $Ca^{2+}$ -ATPase 2
STIM1	Stromal interaction molecule 1
TCGA	The Cancer Genome Atlas

#### Supplementary Information

The online version contains supplementary material available at <https://doi.org/10.1186/s13287-024-03875-1>.

Additional file 1.

Additional file 2.

#### Acknowledgements

We'd like to thank Rajini Rao for her kind gift of SPCA2-N plasmid.

#### Author contributions

XQY initiated the study, designed the experiments, and revised the manuscript; DZ and ZCL designed the experiments, performed most experiments and statistical analysis, and drafted the manuscript; JCL, BBQ performed part of the experiments; XQY, YHT and LWJ provided funding support. AMC, XHJ and LD provided experimental materials and suggestions. All authors read and approved the final manuscript.

### Funding

This work was supported by grants from Hong Kong Research Grant Committee (CRF/C5016-23GF, RIF/R4005-18F) and Innovation and Technology Fund ITS/212/21.

### Data availability

RT-qPCR data, western blot data and all staining data generated in this study are included in this article. All other data are available from the corresponding author upon reasonable request.

### Declarations

#### Ethics approval and consent to participate

Animals were supplied by the University Laboratory Animal Services Centre, and all animal studies were approved by the Animal Experimental Ethics Committee of The Chinese University of Hong Kong. The approved project title: Role of Ca<sup>2+</sup>-permeable channels Orai1 and Orai3 in breast cancer stem cells. Approval number: 20-264-GRF. The date of approval: June 28, 2021. For the patients' samples, the patients or their guardians/legally authorized representatives provided written informed consent for participation in the study and the use of samples. The immunohistochemical experiments using human tissue samples were approved by Ethics Committee of Feicheng Hospital Affiliated to Shangdong First Medical University. The title of the approved project title: Orai1 and Orai3 act through distinct signalling axes to promote stemness and tumorigenicity of breast cancer stem cells. Approval number: 20211001. The date of approval: August 20, 2021.

#### Consent for publication

All authors confirm their consent for publication.

#### Competing interests

The authors declare no competing interests.

#### Author details

<sup>1</sup>School of Biomedical Sciences, The Chinese University of Hong Kong, Shatin, Hong Kong SAR, People's Republic of China. <sup>2</sup>Heart and Vascular Institute and Li Ka Shing Institute of Health Sciences, The Chinese University of Hong Kong, Hong Kong, People's Republic of China. <sup>3</sup>Department of Pathology, National Cancer Center/National Clinical Research Center for Cancer/Cancer Hospital, Chinese Academy of Medical Sciences and Peking Union Medical College, Beijing, People's Republic of China. <sup>4</sup>Centre for Cell and Developmental Biology, State Key Laboratory of Agrobiotechnology, School of Life Sciences, The Chinese University of Hong Kong, Hong Kong, People's Republic of China. <sup>5</sup>Affiliated Hospital (Feicheng) of Shandong First Medical University, Tai'an, People's Republic of China. <sup>6</sup>Department of Biomedical Engineering, The Hong Kong Polytechnic University, Hong Kong, People's Republic of China.

Received: 6 March 2024 Accepted: 4 August 2024

Published online: 13 August 2024

### References

- Harbeck N, Gnant M. Breast cancer. *Lancet*. 2017;389:1134–50.
- Plaks V, Kong N, Werb Z. The cancer stem cell niche: How essential is the niche in regulating stemness of tumor cells? *Cell Stem Cell*. 2015;16:225–38.
- Chalmers SB, Monteith GR. ORAI channels and cancer. *Cell Calcium*. 2018;74:160–7.
- Cantonero C, Sanchez-Collado J, Gonzalez-Nuñez MA, Salido GM, Lopez JJ, Jardin I, et al. Store-independent Orai1-mediated Ca<sup>2+</sup> entry and cancer. *Cell Calcium*. 2019;80:1–7.
- Prakriya M, Lewis RS. Store-operated calcium channels. *Physiol Rev*. 2015;95:1383–436.
- Motiani RK, Abdullaev IF, Trebak M. A novel native store-operated calcium channel encoded by Orai3: selective requirement of Orai3 versus Orai1 in estrogen receptor-positive versus estrogen receptor-negative breast cancer cells. *J Biol Chem*. 2010;285:19173–83.
- Feng M, Grice DM, Faddy HM, Nguyen N, Leitch S, Wang Y, et al. Store-independent activation of Orai1 by SPCA2 in mammary tumors. *Cell*. 2010;143:84–98.
- Tanwar J, Arora S, Motiani RK. Orai3: oncochannel with therapeutic potential. *Cell Calcium*. 2020;90:102247.
- Jardin I, Diez-Bello R, Lopez JJ, Redondo PC, Salido GM, Smani T, Rosado JA. TRPC6 channels are required for proliferation, migration and invasion of breast cancer cell lines by modulation of Orai1 and Orai3 surface exposure. *Cancers*. 2018;10:331.
- Motiani RK, Zhang X, Harmon KE, Keller RS, Matrougui K, Bennett JA, et al. Orai3 is an estrogen receptor  $\alpha$ -regulated Ca<sup>2+</sup> channel that promotes tumorigenesis. *FASEB J*. 2013;27:63–75.
- Yang S, Zhang JJ, Huang XY. Orai1 and STIM1 are critical for breast tumor cell migration and metastasis. *Cancer Cell*. 2009;15:124–34.
- Walsh HR, Cruickshank BM, Brown JM, Marcato P. The Flick of a switch: conferring survival advantage to breast cancer stem cells through metabolic plasticity. *Front Oncol*. 2019;9:753.
- Pal S, Sharma A, Mathew SP, Jananathan BG. Targeting cancer-specific metabolic pathways for developing novel cancer therapeutics. *Front Immunol*. 2022;13:955476.
- Ciavardelli D, Rossi C, Barcaroli D, Volpe S, Consalvo A, Zucchelli M, et al. Breast cancer stem cells rely on fermentative glycolysis and are sensitive to 2-deoxyglucose treatment. *Cell Death Dis*. 2014;5:e1336.
- Chakraborty PK, Mustafa SB, Xiong X, Dwivedi SKD, Nesin V, Saha S, et al. MICU1 drives glycolysis and chemoresistance in ovarian cancer. *Nat Commun*. 2017;8:14634.
- Liu J, Tan Y, Zhang H, Zhang Y, Xu P, Chen J, et al. Soft fibrin gels promote selection and growth of tumorigenic cells. *Nat Mater*. 2012;11:734–41.
- Tan Y, Tajik A, Chen J, Jia Q, Chowdhury F, Wang L, et al. Matrix softness regulates plasticity of tumour-repopulating cells via H3K9 demethylation and Sox2 expression. *Nat Commun*. 2014;5:4619.
- Fathi E, Mesbah-Namin SA, Vietor I, Farahzadi R. Mesenchymal stem cells cause induction of granulocyte differentiation of rat bone marrow C-kit(+) hematopoietic stem cells through JAK3/STAT3, ERK, and PI3K signaling pathways. *Iran J Basic Med Sci*. 2022;25(10):1222–7.
- Li Z, Meng Z, Lu J, Chen FM, Wong WT, Tse G, et al. TRPV6 protects ER stress-induced apoptosis via ATF6 $\alpha$ -TRPV6-JNK pathway in human embryonic stem cell-derived cardiomyocytes. *J Mol Cell Cardiol*. 2018;120:1–11.
- Schiøtz BL, Rosado EG, Baekkevold ES, Lukacs M, Mjaaland S, Sindre H, et al. Enhanced transfection of cell lines from Atlantic salmon through nucleofection and antibiotic selection. *BMC Res Notes*. 2011;4:136.
- Poh YC, Chen J, Hong Y, Yi H, Zhang S, Chen J, et al. Generation of organized germ layers from a single mouse embryonic stem cell. *Nat Commun*. 2014;5:4000.
- Rafat A, Dizaji Asl K, Mazloumi Z, Movassaghpour AA, Talebi M, Shanehbandi D, et al. Telomerase inhibition on acute myeloid leukemia stem cell induced apoptosis with both intrinsic and extrinsic pathways. *Life Sci*. 2022;295: 120402.
- Kwan HY, Huang Y, Yao X. Regulation of canonical transient receptor potential isoform 3 (TRPC3) channel by protein kinase G. *Proc Natl Acad Sci USA*. 2004;101(8):2625–30.
- Wang Y, Li ZC, Zhang P, Poon E, Kong CW, Boheler KR, et al. Nitric Oxide-cGMP-PKG pathway acts on Orai1 to inhibit the hypertrophy of human embryonic stem cell-derived cardiomyocytes. *Stem Cells*. 2015;33:2973–84.
- Zhu Y, Xie M, Meng Z, Leung LK, Chan FL, Hu X, et al. Knockdown of TM9SF4 boosts ER stress to trigger cell death of chemoresistant breast cancer cells. *Oncogene*. 2019;38:5778–91.
- Meng Z, Li Z, Xie M, Yu H, Jiang L, Yao X. TM9SF4 is an F-actin disassembly factor that promotes tumor progression and metastasis. *Nat Commun*. 2022;13(1):5728.
- Wang Q, Armenia J, Zhang C, Penson AV, Reznik E, Zhang L, et al. Unifying cancer and normal RNA sequencing data from different sources. *Sci Data*. 2018;5:180061.
- Elston CW, Ellis IO. Pathological prognostic factors in breast cancer. I. The value of histological grade in breast cancer: experience from a large study with long-term follow-up. *Histopathology*. 1991;19(5):403–10.

29. Beck B, Blanpain C. Unravelling cancer stem cell potential. *Nat Rev Cancer*. 2013;13:727–38.
30. Sadaghiani AM, Lee SM, Odegaard JI, Leveson-Gower DB, McPherson OM, Novick P, et al. Identification of Orai1 channel inhibitors by using minimal functional domains to screen small molecule microarrays. *Chem Biol*. 2014;21:1278–92.
31. Kumari A, Srivastava S, Manne RK, Sisodiya S, Santra MK, Guchhait SK, et al. C12, a combretastatin-A4 analog, exerts anticancer activity by targeting microtubules. *Biochem Pharmacol*. 2019;170:113663.
32. Feng MY, Rao R. New insights into store-independent  $\text{Ca}^{2+}$  entry: secretory pathway calcium ATPase 2 in normal physiology and cancer. *Int J Oral Sci*. 2013;5:71–4.
33. Lu H, Chen I, Shimoda LA, Park Y, Zhang C, Tran L, et al. Chemotherapy-induced  $\text{Ca}^{2+}$  release stimulates breast cancer stem cell enrichment. *Cell Rep*. 2017;18(8):1946–57.
34. Hirata N, Yamada S, Yanagida S, Ono A, Yasuhiko Y, Nishida M, et al. lysophosphatidic acid promotes the expansion of cancer stem cells via TRPC3 channels in triple-negative breast cancer. *Int J Mol Sci*. 2022;23(4):1967.
35. Jardin I, Lopez JJ, Sanchez-Collado J, Gomez LJ, Salido GM, Rosado JA. Store-operated calcium entry and its implications in cancer stem cells. *Cells*. 2022;11(8):1332.
36. Lee SH, Rigas NK, Lee CR, Bang A, Srikanth S, Gwack Y, et al. Orai1 promotes tumor progression by enhancing cancer stemness via NFAT signaling in oral/oropharyngeal squamous cell carcinoma. *Oncotarget*. 2016;7:43239–55.
37. Terrié E, Déliot N, Benzidane Y, Harnois T, Cousin L, Bois P, et al. Store-operated calcium channels control proliferation and self-renewal of cancer stem cells from glioblastoma. *Cancers (Basel)*. 2021;13:3428.
38. Daya HA, Kouba S, Ouled-Haddou H, Benzerdjeb N, Telliez MS, Dayen C, et al. Orai3 mediates cisplatin-resistance in non-small cell lung cancer cells by enriching cancer stem cell population through PI3K/AKT pathway. *Cancers (Basel)*. 2021;13:2314.
39. Farahzadi R, Valipour B, Fathi E, Pirmoradi S, Molavi O, Montazersaheb S, et al. Oxidative stress regulation and related metabolic pathways in epithelial-mesenchymal transition of breast cancer stem cells. *Stem Cell Res Ther*. 2023;14(1):342.
40. Monteith GR, Prevarskaya N, Roberts-Thomson SJ. The calcium-cancer signalling nexus. *Nat Rev Cancer*. 2017;17:367–80.
41. Vaeth M, Maus M, Klein-Hessling S, Freinkman E, Yang J, Eckstein M, et al. Store-operated  $\text{Ca}^{2+}$  entry controls clonal expansion of T cells through metabolic reprogramming. *Immunity*. 2017;47:664–79.e6.
42. Wu W, Wang X, Liao L, Chen J, Wang Y, Yao M, et al. The TRPM7 channel reprograms cellular glycolysis to drive tumorigenesis and angiogenesis. *Cell Death Dis*. 2023;14(3):183.
43. Liu X, Wan X, Kan H, Wang Y, Yu F, Feng L, et al. Hypoxia-induced upregulation of Orai1 drives colon cancer invasiveness and angiogenesis. *Eur J Pharmacol*. 2018;832:1–10.
44. Dai X, Cheng H, Bai Z, Li J. Breast cancer cell line classification and its relevance with breast tumor subtyping. *J Cancer*. 2017;8:3131–41.
45. Rodriguez D, Ramkairsingh M, Lin X, Kapoor A, Major P, Tang D. The central contributions of breast cancer stem cells in developing resistance to endocrine therapy in estrogen receptor (ER)-positive breast cancer. *Cancers (Basel)*. 2019;11:1028.
46. Cuzick J. Predicting late recurrence in ER-positive breast cancer. *Nat Rev Clin Oncol*. 2019;16:406–8.

## Publisher's Note

Springer Nature remains neutral with regard to jurisdictional claims in published maps and institutional affiliations.